

# Ionospheric HF pump wave triggering of local auroral activation

N. F. Blagoveshchenskaya,<sup>1</sup> V. A. Kornienko,<sup>1</sup> T. D. Borisova,<sup>1</sup> B. Thidé,<sup>2</sup>  
M. J. Kosch,<sup>3</sup> M. T. Rietveld,<sup>3</sup> E. V. Mishin,<sup>4</sup> R. Y. Luk'yanova,<sup>1</sup>  
and O. A. Troshichev<sup>1</sup>

**Abstract.** Experimental results from ionospheric HF pumping experiments in the nightside auroral *E* region above Tromsø are reported. We found intriguing evidence that a modification of the ionosphere-magnetosphere coupling, due to the effects of powerful HF waves beamed into an auroral sporadic *E* layer, can lead to a local intensification of the auroral activity. Summarizing multi-instrument observations during two consecutive nights, one can distinguish the following peculiarities related to this auroral activation: a modification of the auroral arc and its breakup above Tromsø, local changes in the horizontal currents above Tromsø, a burst-like increase of the electron density and temperature, a large increase in the ion temperature in a wide altitude range and in the north-south component of the electric field, distinctive features in dynamic HF radio scatter Doppler spectra, pump-induced electron precipitation, and substorm activation exactly above Tromsø. We discuss the modification of the ionosphere-magnetosphere coupling in terms of the excitation of a turbulent Alfvén boundary layer between the base of the ionosphere ( $\sim 100$  km) and the level of sharp increase of the Alfvén velocity (at heights up to one Earth radius), and the formation of a local magnetospheric current system. The results suggest that a possible triggering of local auroral activation requires specific geophysical conditions.

## 1. Introduction

Field-aligned currents (FACs) play an important role in the process of energy transfer between the magnetosphere and the ionosphere. They establish the force balance between the hot, tenuous plasma of the magnetosphere and the cold, dense plasma of the ionosphere [Haerendel, 1990]. Important agents in the magnetosphere-ionosphere coupling are Alfvén waves, since they are equivalent to time-varying field-aligned currents. It has been suggested that the static coupling is dominant for large-scale magnetosphere-ionosphere coupling, while the Alfvén wave coupling is dominant for small-scale coupling [Nagatsuma *et al.*, 1996; Stasiewicz *et al.*, 2000].

One of the most remarkable manifestations of the dynamic processes in the solar wind-magnetosphere-ionosphere system is the substorm phenomenon. It is known that a magnetospheric substorm involves two components: the directly driven component and the energy storage release part. The driven system responds directly to changes in the interplanetary medium (interplanetary magnetic field (IMF)

orientation and solar wind pressure) and involves the direct deposition of solar wind energy into the auroral ionosphere and the symmetric ring currents. The storage-release system pertains to the process of storage of energy in the tail magnetic field and in the kinetic drift of the magnetotail particles. After that, the energy is explosively released into the auroral ionosphere and symmetric ring current system [Rostoker *et al.*, 1987; Rostoker, 1999]. As pointed out by Rostoker [1999], the progress of the substorm may be produced by either a more global, directly driven process or a more localized, storage-release process and may be looked at either on a global scale or on a local scale.

During a substorm onset, the large-scale laminar magnetospheric convection is disrupted because the magnetospheric cross-tail current is diverted down the magnetic field lines [McPherron *et al.*, 1973]. This leads to the activation of the substorm current loop, the so-called substorm current wedge [Kamide and Baumjohann, 1993; Rostoker *et al.*, 1987]. Boström [1964] proposed two auroral current systems connected to the auroral electrojet. This model has not only remained valid up to present time but also comprises most suggestions made later on.

At the ionospheric level the substorm expansion onset is characterized by a brightening and a subsequent breakup of a preexisting auroral arc [Akasofu, 1964]. There are indications that some auroral arcs are generated by field line resonances (FLRs) [Samson *et al.*, 1996].

Lui and Murphree [1998] proposed a substorm onset model by combining a theory of the auroral arc generation due to FLRs with a theory of current disruption in the near-Earth magnetic tail based on the cross-field current instability. This allows a close tie between the current disruption

<sup>1</sup>Arctic and Antarctic Research Institute, St. Petersburg, Russia.

<sup>2</sup>Swedish Institute of Space Physics, Uppsala Division, Uppsala, Sweden.

<sup>3</sup>Max-Planck-Institut für Aeronomie, Katlenburg-Lindau, Germany.

<sup>4</sup>Haystack Observatory, Massachusetts Institute of Technology, Westford, Massachusetts.

region in the magnetotail and the location of the auroral arc.

In recent times, it has been generally assumed that the ionosphere plays a rather passive role in the substorm process. Nonetheless, some exceptions to this assumption exist. Firstly, the models proposed by *Kan and Sun* [1985], *Kan* [1993], and *Lysak* [1990] emphasize changes in the ionospheric conductivity and its role in enhancing the field-aligned currents [*Lysak and Song*, 1998]. Secondly, there exist models which emphasize the decoupling of magnetospheric convection from the ionosphere, induced by the formation of parallel electric fields [*Haerendel*, 1990]. Lastly, there are models which emphasize the excitation of a turbulent Alfvén boundary layer in the polar ionosphere, thus giving rise to a strong turbulent heating of the plasma and to the production of accelerated particles [*Trakhtengerts and Feldstein*, 1991].

To investigate, in a systematic and repeatable fashion, the role of the auroral ionosphere in the substorm process, a controlled injection of high-power radio waves into space from purpose-built ground-based HF radio facilities constitutes an excellent tool. This “stimulus-response” type of experimental technique is well known from ground-based laboratories and is now also well established in space.

Experimental results concerning the possibility of an artificial modification of the ionosphere-magnetosphere system by HF radio waves were presented by *Blagoveshchenskaya et al.* [1998, 1999]. In the present paper we report experimental results from Tromsø HF pumping experiments in the nightside auroral  $E$  region, and we present evidence for a modification, produced by the powerful HF radio waves, of the ionosphere-magnetosphere coupling, leading to a local intensification of the auroral activity. Data from bistatic HF Doppler radio scatter, the International Monitor for Auroral Geomagnetic Effects (IMAGE) magnetometer network, the European Incoherent Scatter (EISCAT) UHF radar, the Tromsø dynasonde, the digital all-sky imager (DASI), and the IMP 8 and IMP 9 satellites were used in the analysis.

## 2. Experimental Methods and Equipment Used

The experiments reported here were conducted by using the EISCAT HF heating facility [*Rietveld et al.*, 1993] located near Tromsø (geographical coordinates  $69.6^\circ\text{N}$ ,  $19.2^\circ\text{E}$ ,  $L = 6.2$ , magnetic dip angle  $I = 78^\circ$ ) in the pre-midnight hours of February 16 and 17, 1996. The Tromsø heater was operating at the frequency 4040 kHz,  $O$  mode polarization, with an effective radiated power of 150 MW. The antenna beam was tilted  $6^\circ$  to the south, thus allowing HF pumping in a near-field-aligned direction.

Bistatic scatter measurements of HF diagnostic signals were carried out on the London–Tromsø–St. Petersburg path at operational frequencies of 9410 and 12,095 kHz. The analysis of the received diagnostic waves, scattered from artificial field-aligned irregularities (AFAIs) above Tromsø, was made with a Doppler spectral method in St. Petersburg at a distance of  $\sim 1200$  km; the receiving antenna was directed toward Tromsø. The geometry of the experiments is shown in Figure 1. Spectral processing of the diagnostic sig-

nals was made with a fast Fourier transform (FFT) method. On February 16 and 17 the frequency bandwidth used was 50 and 33 Hz, respectively, with a frequency resolution of  $\sim 0.1$  Hz and a temporal resolution of  $\sim 10$  s.

To facilitate the interpretation of the Doppler measurements, we used data from the IMAGE magnetometer network [*Lühr et al.*, 1998]. The locations of the IMAGE magnetometers are depicted in Figure 1. The temporal resolution of the IMAGE magnetometers used in this study was 10 s.

Information about disturbances in the interplanetary magnetic field (IMF) and in the solar wind, which could be related to the substorm onset, was obtained from IMP 8 and IMP 9 satellite data. The temporal resolution of the satellite data used in this study was 1 min.

Optical data were obtained with the digital all-sky imager (DASI). Details of the instrumentation can be found in the work by *Kosch et al.* [1998]. The DASI is located at Skibotn, near Tromsø ( $69.3^\circ\text{N}$ ,  $20.4^\circ\text{E}$ ). In this study we used 557.7-nm data with 10- and 30-s temporal resolution.

To obtain information about changes in the electron densities and temperatures,  $N_e$  and  $T_e$ , and the ion temperatures and velocities,  $T_i$  and  $V_i$ , during HF pumping experiments, EISCAT UHF radar [*Rishbeth and van Eyken*, 1993] measurements in the field-aligned direction above Tromsø were employed.

## 3. Observational Results

The Tromsø dynasonde ionograms as well as the altitude-temporal variations of the electron density measured by the EISCAT UHF radar in the course of the Tromsø pumping experiments on February 16 and 17, 1996, show the presence of an intense auroral  $E_s$  layer with a maximum plasma frequency of  $4.1 \leq f_oE_s \leq 4.5$  MHz at heights  $100 \leq h_mE_s \leq 110$  km. We therefore conclude that the  $E$  region of the auroral ionosphere was actually the region where the powerful HF radio waves were reflected. This led to the generation of AFAIs, which scattered the 9- and 12-MHz signals used for Doppler diagnostics. It is believed [*Djuth et al.*, 1985; *Noble et al.*, 1987] that a thermal resonance instability at the upper hybrid (UH) level is the strongest candidate for the excitation of AFAIs in the  $E$  region.

It should be noted that under the specific conditions during the experiments with a pump wave at 4040 kHz reflecting off an overdense auroral  $E_s$  layer, the  $O$  mode HF sets up a standing wave. As shown by *Lundborg and Thidé* [1986], the amplitude swelling of the electric field strength of such a standing wave can be very high at and immediately below the reflection altitude (plasma resonance region) for an overdense  $E_s$  layer. In our experiments this altitude happens to coincide with the altitude of the auroral electrojet. Hence, in the experiments reported here the conductivity in the electrojet is expected to increase owing to the HF pump action; see the review article by *Stubbe* [1996].

### 3.1. Experiment on February 17, 1996

The experiment on February 17, 1996, was conducted from 2000 to 2300 UT by using a 4 min on, 6 min off HF

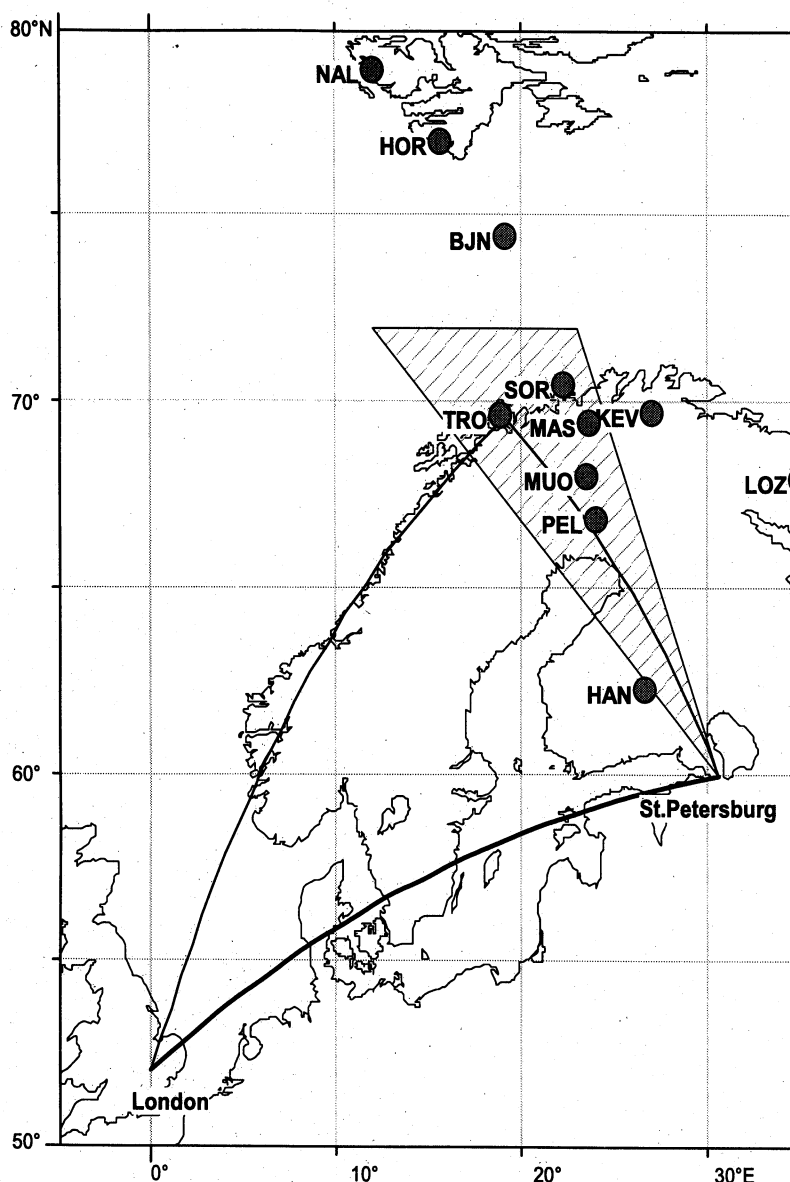


**Figure 1.** General view of the experiment geometry, indicating the position of the London–Tromsø–St. Petersburg path, where HF Doppler measurements of the HF signals scattered from artificial field-aligned irregularities (FAIs) were made, and the locations of the International Monitor for Auroral Geomagnetic Effects (IMAGE) magnetometer stations. The names of the stations used are as follows: Ny Ålesund (NAL; 78.92°N, 11.95°E), Hornsund (HOR; 77.00°N, 15.60°E), Bear Island (BJN; 74.50°N, 19.20°E), Sørøya (SOR; 70.54°N, 22.22°E), Tromsø (TRO; 69.66°N, 18.94°E), Masi (MAS; 69.46°N, 23.70°E), Muonio (MUO; 68.02°N, 23.53°E), Pello (PEL; 66.90°N, 24.08°E), Hankasalmi (HAN; 62.30°N, 26.65°E), Kevo (KEV; 69.76°N, 27.01°E), and Lovozero (LOZ; 67.97°N, 35.08°E).

cycle. A very interesting observation in this experiment is the behavior of the auroral arc in the vicinity of Tromsø during the heating cycle 2030–2034 UT; see the DASI data in Plate 1. Beginning at 2032 UT (third row in Plate 1), a gradual thinning of the auroral arc, accompanied by the appearance of a weak bulge above Tromsø, is observed. Thereafter, the brightening and subsequent breakup of the arc at 2033:40 UT takes place exactly above Tromsø.

The magnetic field  $X$ ,  $Y$ , and  $Z$  components, as recorded by the Ny Ålesund (NAL), Hornsund (HOR), Bear Island (BJN), Sørøya (SOR), Tromsø (TRO), Masi (MAS), Muonio (MUO), Pello (PEL), and Hankasalmi (HAN) stations of the

IMAGE magnetometer network, are displayed in Figure 2; see also Figure 1. It can be seen that a substorm activation started at 2000 UT. A second activation started at 2033 UT, indicated by a large negative spike in the magnetic  $X$  component, localized in a narrow latitudinal region around Tromsø, from the SOR station to the MAS station.

Examination of the peculiarities in the behavior of the  $X$  and  $Z$  magnetic components in Figure 2 shows that a new westward electrojet appeared at 2033 UT exactly above Tromsø (reversal of the  $Z$  component from positive values at SOR to negative values at MAS, with  $Z \approx 0$  at the TRO station), and maximal negative amplitude of the  $X$  component

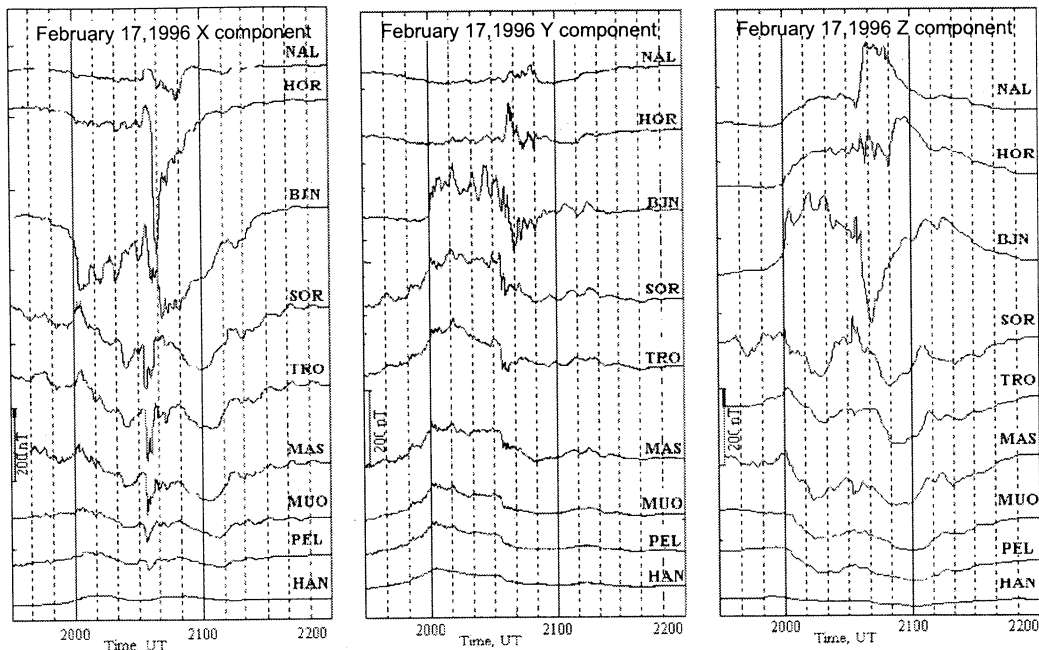


**Figure 2.** The temporal behavior of the X, Y, and Z components of the magnetic field variations on February 17, 1996. Data are from the IMAGE magnetometers.

( $X_{max} = -130$  nT at Tromsø). Thereafter, at 2038 UT a large substorm started at higher latitudes ( $X_{max} = -400$  nT at the HOR station). We will only consider the substorm activation around Tromsø, which started at 2033 UT.

Studies of magnetograms from the Kevo (Figure 3) and Lovozero (Figure 4) stations, which are both located further east of Tromsø, clearly show that the intensity of the magnetic disturbance is decreasing with distance from Tromsø. Hence we can safely conclude that the substorm really occurred above Tromsø.

The behavior of the equivalent current vectors (from the X and Y magnetic components in Figure 2), describing the distribution of the magnetic disturbances from 2029 to 2036 UT, is summarized in Figure 5. As is clearly seen, the most drastic changes of the current directions and magnitudes in the vicinity of Tromsø from SOR to MAS took place during the period 2033–2034 UT.

It is well established that the onset of a substorm can be related to disturbances in the interplanetary magnetic field (IMF) and/or in the solar wind. Consequently, it is of inter-

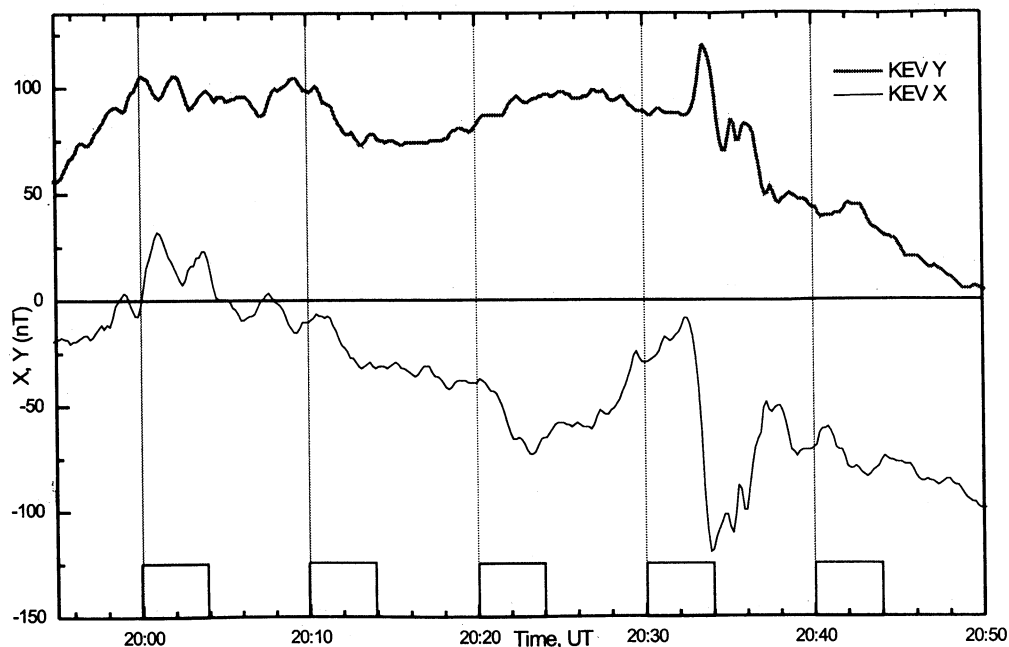


**Figure 3.** Magnetic X and Y components measured at the Kevo (KEV) magnetic station on February 17, 1996, from 1955 to 2050 UT. The heater-on periods are indicated on the bottom axis.

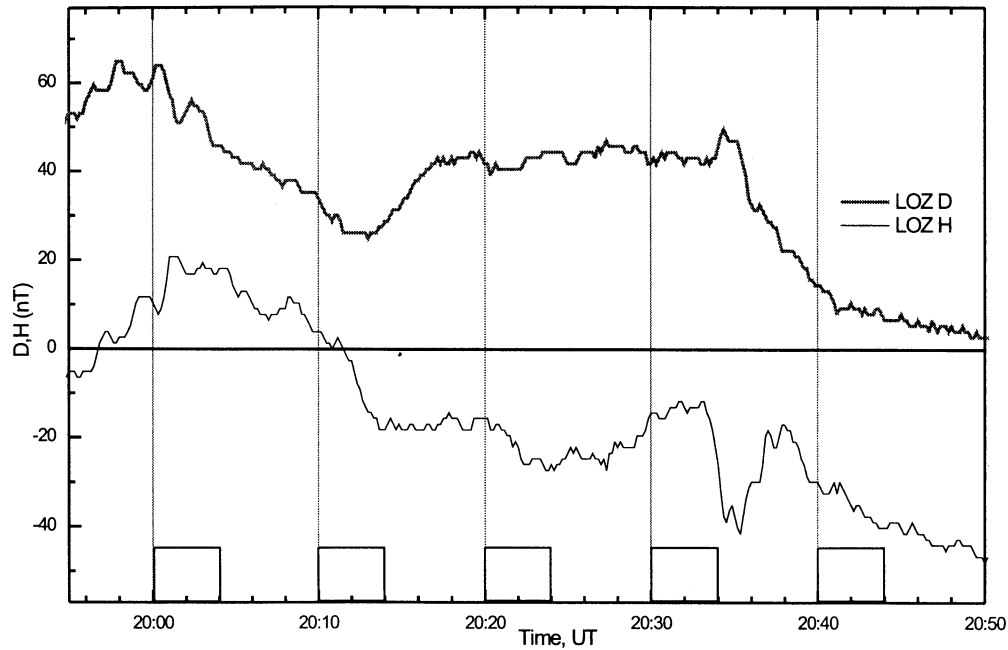


**Figure 4.** Magnetic  $H$  and  $D$  components measured at the Lovozero (LOZ) magnetic station on February 17, 1996, from 1955 to 2250 UT. The heater-on periods are indicated on the bottom axis.

est to consider IMF and solar wind data for the time intervals during which the HF pumping experiments were carried out. The behavior of the  $B_x$ ,  $B_y$ , and  $B_z$  components of the IMF as well as the solar wind velocity  $V$  from IMP 8 and IMP 9 satellite data shows that there were no significant changes in the  $B_z$  and  $B_y$  components; during the period 1600–2200 UT they underwent maximal amplitude fluctuations not exceeding 1.5 nT. Nonetheless, it should be pointed out that small directional changes in the  $B_z$  component (northward turning) accompanied by a  $B_x$  turn from positive to negative values occurred at about 2035 UT. Therefore IMF data show an absence of major directional changes in the  $B_z$  and  $B_y$  components which could be associated with the auroral activation at 2033:40 UT. In this respect, we note the results of detailed observations performed by *Henderson et al.* [1996] which show that a magnetospheric substorm can indeed occur in the absence of an identifiable driver in either the IMF or the solar wind dynamic pressure. It is suggested that the internal instability in the magnetospheric system could be the possible driver for these substorms.

Figure 6 presents dynamic Doppler spectra of HF diagnostic signals recorded in St. Petersburg in the course of three heating cycles from 2008 to 2038 UT. The turning on of the Tromsø heater at 2010 and 2020 UT led to the appearance of two additional tracks, shifted from the direct signal by about  $-2.5$  Hz. These additional tracks disappeared after the heater was turned off at 2014 and 2024 UT, respectively, and were produced by diagnostic waves scattered off HF pump-induced field-aligned irregularities (AFIs) in the  $E$  region above Tromsø.

As can also be seen from Figure 6, the heater turn-on at 2030 UT led to the appearance of field-aligned scattered HF signals in the same manner as in the preceding heating cy-

cles. About 60 s later, a wideband spectral feature occurred throughout the spectral bandwidth analyzed. Thereafter, at 2033 UT, an additional, very intense, short-lived track of  $\sim 1$  min duration, displaced  $-0.8$  Hz from the main scattered signal, appeared in the Doppler sonogram. The heater turn-off at 2034 UT was followed by the disappearance of an additional short-lived track, but the AFI-scattered signals, as well as the wideband spectral features, were maintained for yet another minute.

What is the nature of the wideband spectral feature closely linked to the auroral activation? It is known that one of the most common features in HF pumping experiments is the generation of Stimulated Electromagnetic Emissions (SEE) [Thidé *et al.*, 1982, 1983, 1989; Thidé, 1990; Stubbe *et al.*, 1984; Leyser *et al.*, 1994]. Unfortunately, no SEE diagnostics capability was available during the experiments, so it was not possible to establish directly whether SEE were excited or not. However, numerous SEE experiments performed over the years enable us to claim, on statistical grounds, that the probability is very high that SEE were indeed excited. The occurrence of SEE is, in turn, a manifestation of turbulent, nonlinear interactions between plasma modes of high and low frequencies.

Therefore a possible explanation for the observed heater-related wideband features is the excitation of VLF waves and turbulence by the ionospheric HF pump wave. Indeed, *Vas'kov et al.* [1998] concluded, from satellite experiments during the action of unmodulated powerful HF radio waves on the nightside ionospheric  $F$  region, that VLF waves may be excited owing to a decay process taking place near the pump wave reflection region or owing to the interaction with suprathermal electrons, accelerated by the pump-enhanced plasma turbulence. The heater-induced VLF waves can be

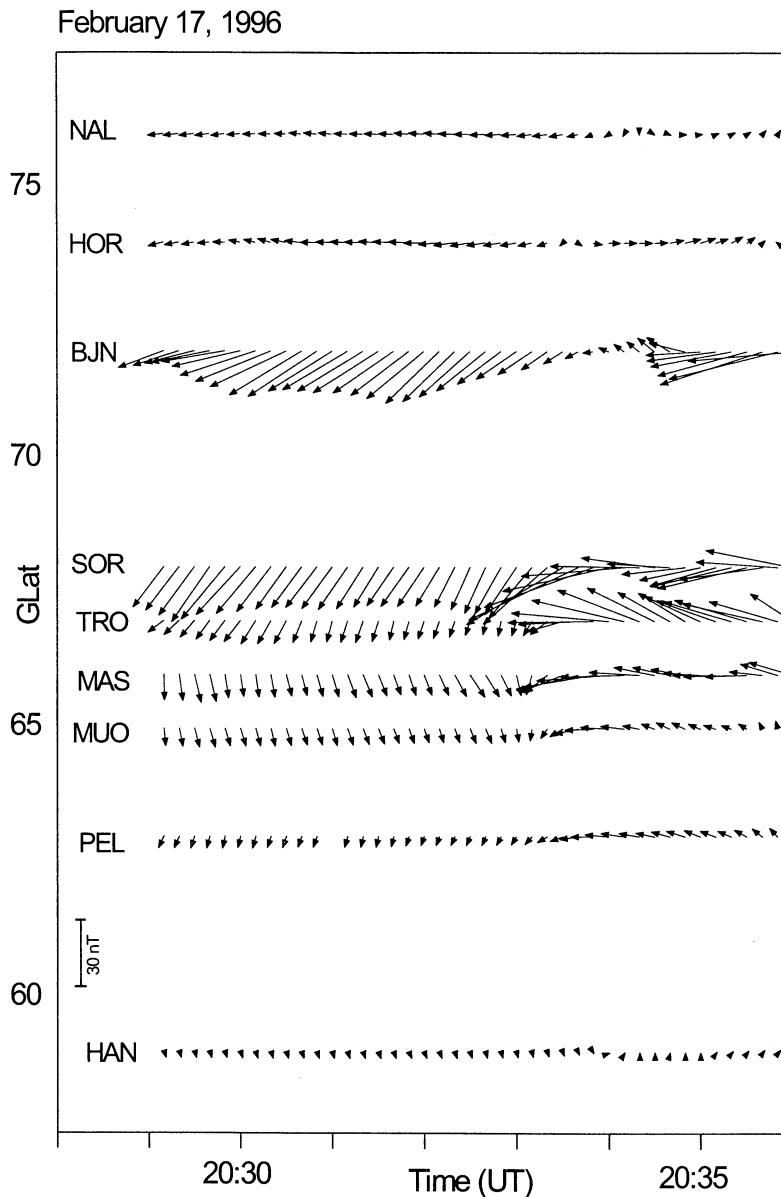


**Figure 5.** The behavior of the equivalent current vectors on February 17, 1996, from 2029 to 2036 UT, describing the distribution of magnetic disturbances at the IMAGE network. The heater-on period was from 2030 to 2034 UT.

studied by ground-based techniques. Also, HF-excited VLF waves in the whistler mode were detected by satellites in the upper ionosphere and magnetosphere within the magnetic flux tube footprinted on the heating facility [Vas'kov *et al.*, 1998].

However, the long-delayed effect of  $\sim 1$  min duration, of the wideband feature observed after the heater turn-off, is not easy to explain. Because of this, we do not exclude the possibility that this emission in our experiment is a heater-modified natural auroral emission in the decameter range [LaBelle *et al.*, 1995; Weatherwax *et al.*, 1995].

Closely related to the wideband spectral features in the probe wave sidebands was the appearance of an additional short-lived track in the Doppler sonogram. It is likely that this short-lived track was induced by a stimulated precipitation of electrons due to a cyclotron resonant interaction of

natural precipitating electrons with heater-induced whistler waves in the magnetosphere [Trefall *et al.*, 1975; Bösinger *et al.*, 1996]. From the results obtained we may then conclude that the substorm activation on February 17, 1996, at 2033 UT above Tromsø was initiated by pump-induced electron precipitation.

EISCAT Tromsø UHF radar data ( $N_e$ ,  $T_e$ ,  $T_i$ , and  $V_i$ ) obtained on February 17, 1996, are displayed in Plate 2. Plate 2 shows the occurrence of a burst-like increase of the electron density and temperature,  $N_e$  and  $T_e$ , in a wide range of altitudes at 2033 UT. The observed changes in the  $N_e$  and  $T_e$  are closely correlated with the auroral activation and may therefore be a signature of heater-induced precipitation of electrons.

Summarizing the experimental findings from the different ground-based measurements during the heater-on period

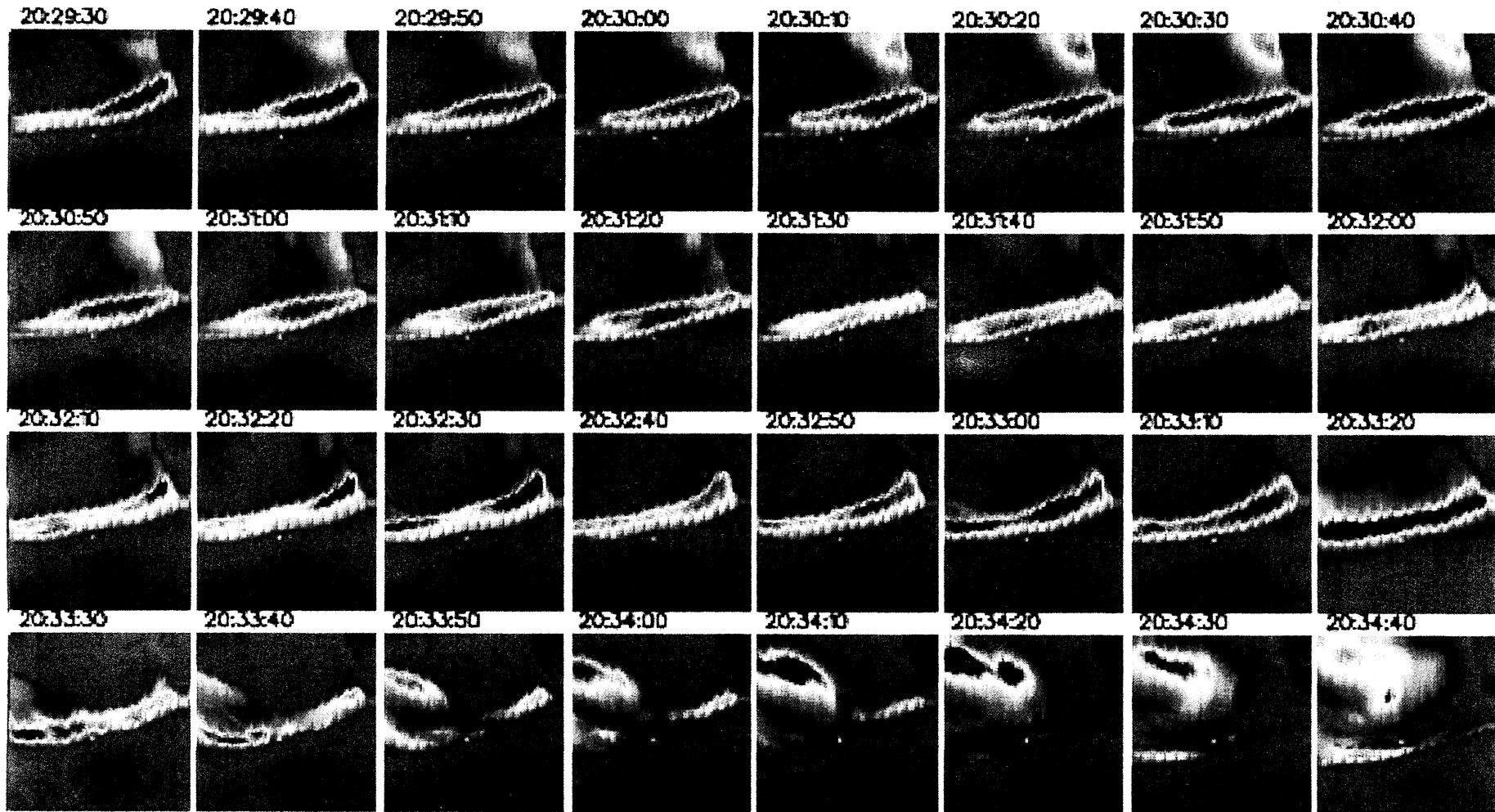


**Plate 1.** A sequence of all-sky imager plots at 557.7 nm obtained near Tromsø on February 17, 1996, from 2029:30 to 2034:40 UT. The spatial scale of each plot is  $520 \times 520 \text{ km}^2$ . The white point near the middle of each plot indicates the location of Tromsø. The plot time is 10 s. The Tromsø heater was turned on from 2030 to 2034 UT.

## EISCAT UHF radar, Tromsø, 17 February 1996

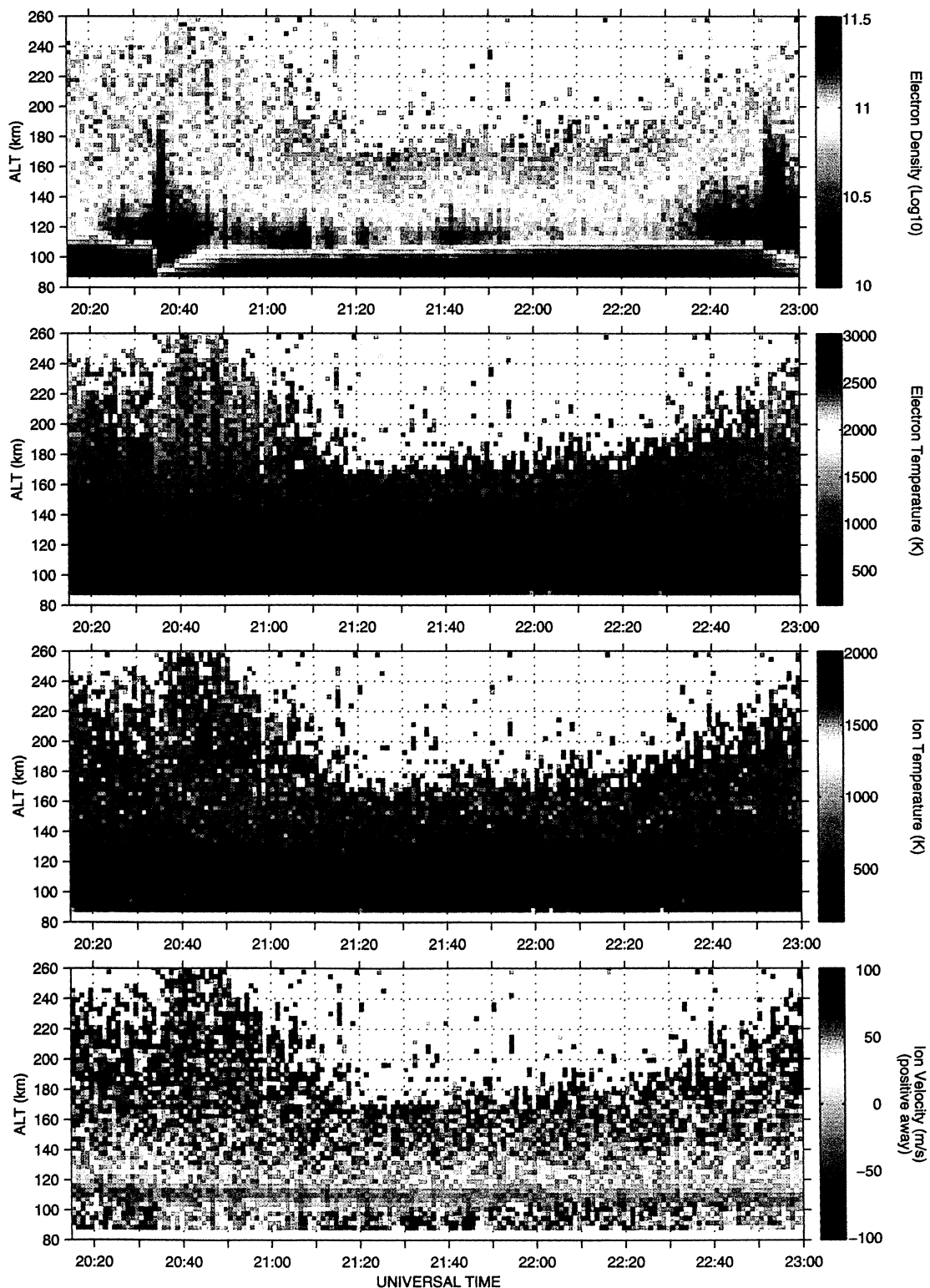


**Plate 2.** Behavior of the electron density, electron and ion temperatures, and ion velocity as observed with the Tromsø EISCAT UHF incoherent scatter radar in the field-aligned direction on February 17, 1996, from 2015 to 2300 UT, by using a high spatial resolution alternating code (AC). The Tromsø HF heating facility was operated from 2020 to 2300 UT with a 4 min on, 6 min off pump cycle.



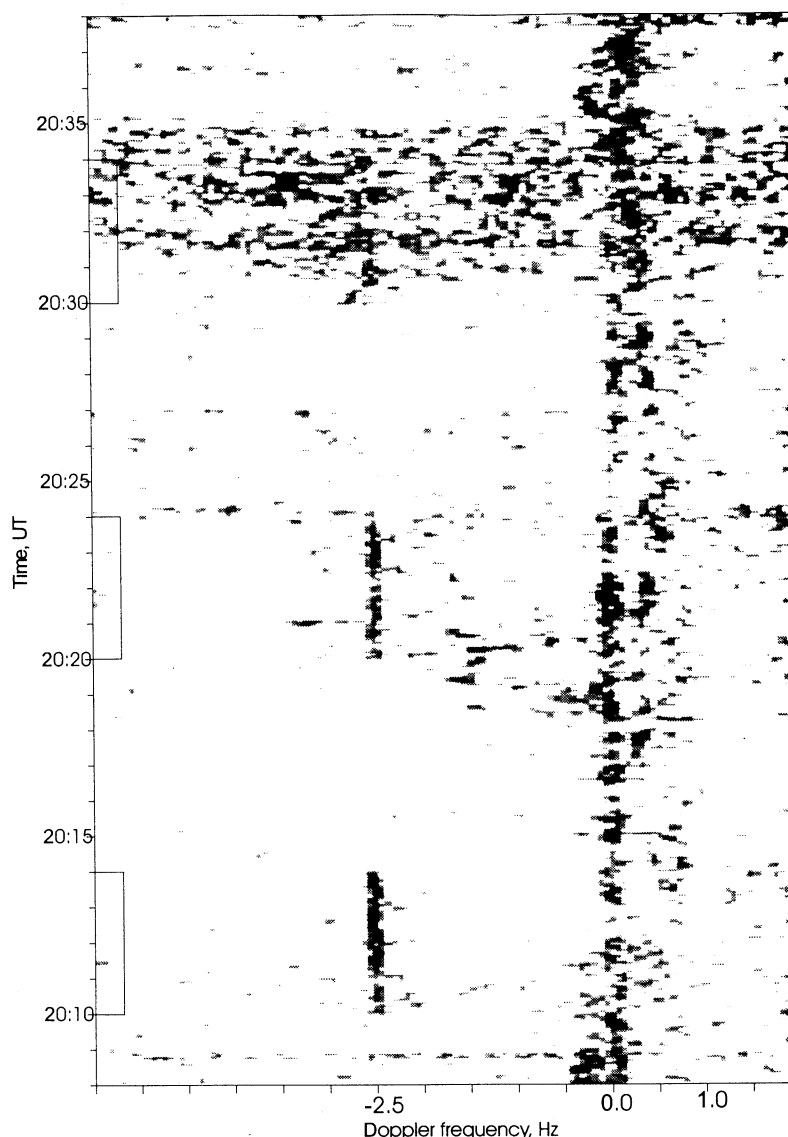


**Figure 6.** Dynamic Doppler spectra of HF diagnostic signals on the London–Tromsø–St. Petersburg path at the operational frequency 12,095 kHz on February 17, 1996, from 2008 to 2038 UT. The direct signals propagating from the transmitter to the receiver along a great circle path correspond to zero Doppler shifts. The intervals when the Tromsø heater was turned on are marked on the time axis.

of 2030–2034 UT on February 17, one can distinguish the following peculiarities related to the auroral activation observed within 30 min after the start of the pumping experiment in the absence of apparent drivers in the IMF/solar wind parameters: (1) a modification of the auroral arc and its breakup above Tromsø; (2) local changes of the horizontal currents in the  $E$  region; (3) a generation of scattered Doppler components throughout the whole spectral bandwidth of 33 Hz analyzed; (4) the appearance of an additional short-lived Doppler sonogram track, distinct from the main track, corresponding to scattered diagnostic signals due to pump-induced electron precipitation; (5) a burst-like increase of  $N_e$  and  $T_e$  in a wide altitude range; and (6) substorm activation exactly above Tromsø.

### 3.2. Experiment on February 16, 1996

In this section we present data from the Tromsø HF pumping experiment carried out on February 16, 1996, starting at 2100 UT. The pump wave was modulated with a 4 min on, 6 min off cycle from 2100 to 2300 UT. This was preceded by some short on periods as the HF transmitter was tuned, from 2041 to 2044 UT, from 2046:30 to 2048:30 UT, and from 2052:00 to 2052:20 UT. The DASI digital all-sky imager data for this day (Plate 3) show that an east-west directed auroral arc was located slightly to the south of the heater. It should be pointed out that a most remarkable optical phenomenon was observed during the two heating cycles of 2120–2124 and 2130–2134 UT. As can be seen in

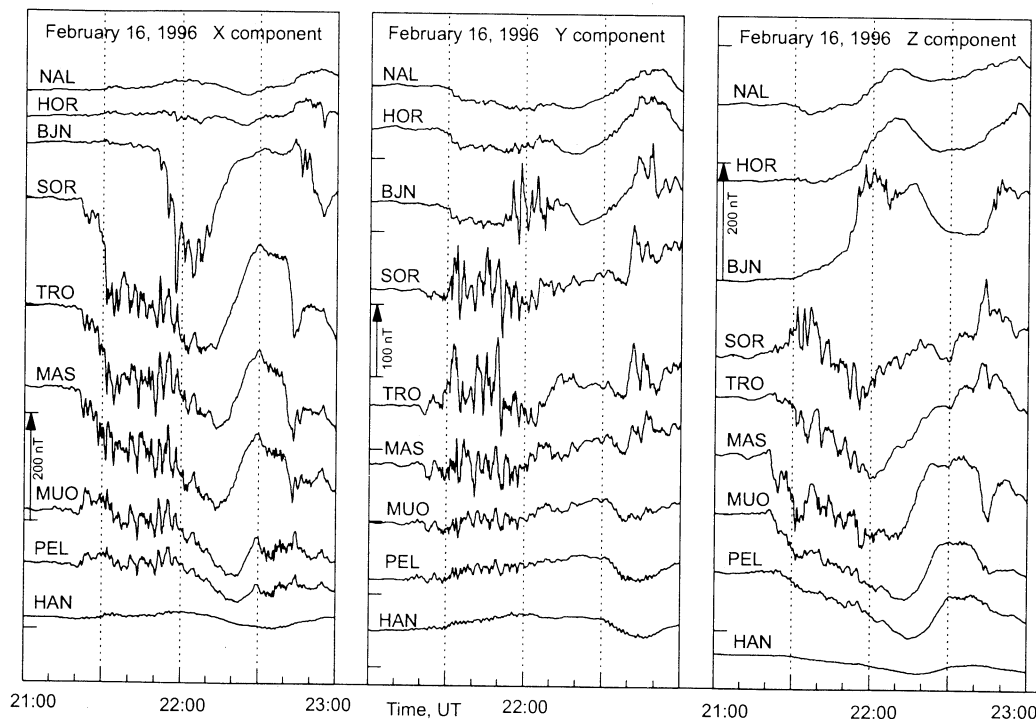


**Figure 7.** The temporal behavior of the X, Y, and Z components of the magnetic field variations on February 16, 1996. Data are from the IMAGE magnetometers.

Plate 3, local spiral-like forms developed in the auroral arc near Tromsø occurred after the heater was turned on. In the first case (2120–2124 UT) the spiral form appeared at 2121:50 UT and led to the start of an auroral activation. In the course of the heater-on period the intensity of this spiral increased and started to decay only after the heater was turned off. In the second case (2130–2134 UT) a similar form, but more intense in comparison with the heater-on period of 2120–2124 UT, appeared at 2131:20 UT. Furthermore, the brightening and subsequent breakup of an auroral arc at 2133:50 UT (Plate 3, fourth row, last panel) took place exactly above Tromsø. Such a spiral form can be attributed to the local appearance of field-aligned currents during the heater-on periods of 2120–2124 and 2130–2134 UT.

IMAGE magnetograms for the event on February 16, 1996 (X, Y, and Z magnetic components), are displayed in Figure 7. These magnetic data indicate that the Tromsø heater operation started under quiet magnetic conditions (from 2100 UT) and that the start of the auroral activation occurred at 2121 UT, during the third heating cycle (2120–2124 UT). It should be noted that this event, just as the auroral activation on February 17, 1996, occurred in a narrow latitudinal region localized around Tromsø, as is evident from the behavior of the equivalent current vectors obtained from the IMAGE magnetometers from 2119 to 2127 UT (Figure 8). Moreover, the most drastic changes of the current directions and magnitudes were also observed in the vicinity of Tromsø, ranging in latitude from the SOR to the MAS magnetic stations.

The  $B_x$ ,  $B_y$ , and  $B_z$  components of the IMF and the solar wind velocity obtained from IMP 8 and IMP 9 satellite data for the event on February 16, 1996, show, contrary to the

event on February 17, that a southward turning of the  $B_z$  component of the IMF took place at 2040 UT. The amplitude of the southward  $B_z$  component was about  $-2$  nT. This small directional change in the  $B_z$  component could possibly be a driver for the auroral activation.

Figure 9 displays the dynamic Doppler spectra obtained on February 16, 1996, from 2058 to 2140 UT, on the London–Tromsø–St. Petersburg path, for a radio scatter operational frequency of  $f = 9410$  kHz. One can see that the spectral structure of the signals scattered from AFAIs is quite complicated, including a broadening of the Doppler spectra and burst-like noise enhancements. The variations of the Doppler frequency with time of the broad part in the dynamic Doppler spectra can be correlated with the movements of the auroral arcs around Tromsø on the line of sight of the radio scatter observations from St. Petersburg. Note that the scattered signals were observed from both natural and artificial ionospheric irregularities during the HF pumping experiment on February 16, 1996. This is in contrast to the experiment on February 17, 1996, when only well-defined artificial irregularities, closely related to heater-on periods, were observed from 2000 to 2100 UT.

The noise enhancement occurred over a frequency range of up to 35 Hz, which is below the  $O^+$  ion cyclotron frequency of 47 Hz. We emphasize that the Doppler measurements in this modification experiment were performed in a limited frequency bandwidth of 50 Hz. At frequencies below the ion cyclotron frequency the only known electromagnetic mode of propagation along magnetic field lines is the Alfvén wave. Thus one would expect that Alfvén waves would be excited by the HF pumping of the nightside auroral E region. Alfvén waves associated with ELF noise are identified with

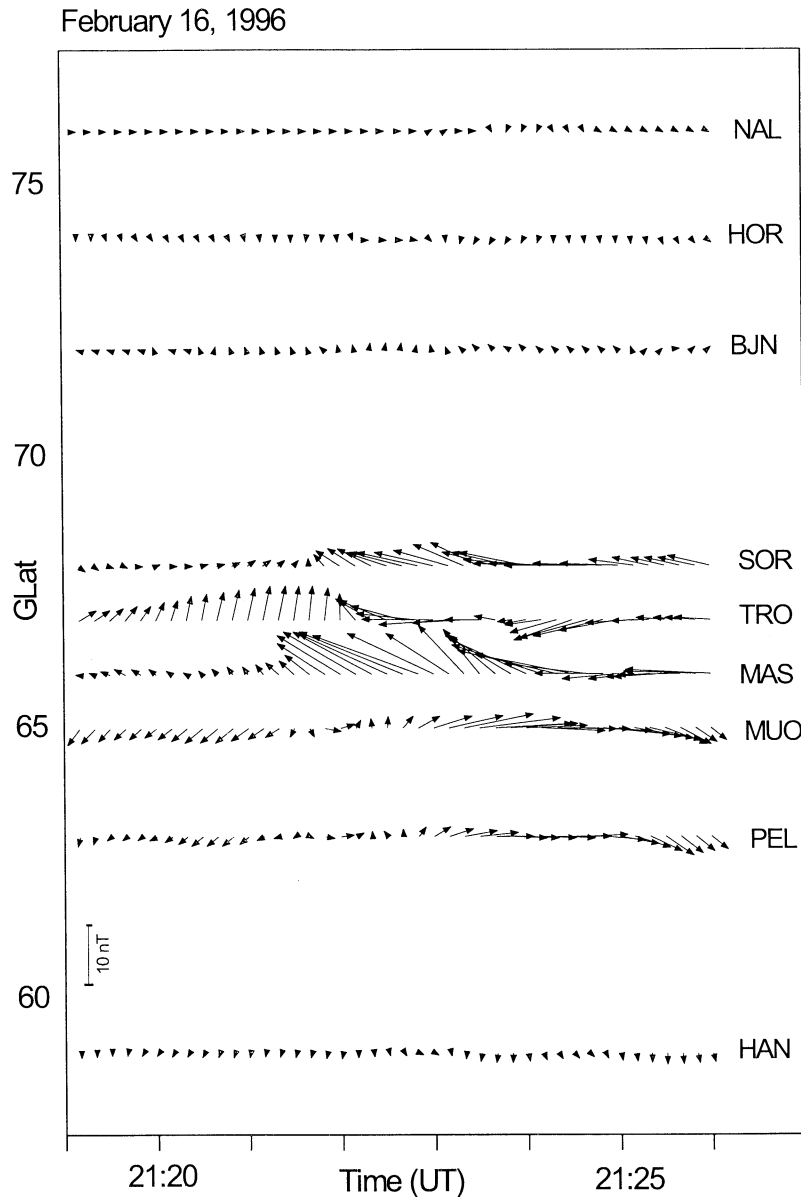


**Figure 8.** The behavior of the equivalent current vectors on February 16, 1996, from 2119 to 2127 UT, describing the distribution of magnetic disturbances at the IMAGE network. The heater-on period was from 2120 to 2124 UT.

electric to magnetic field ratios of the order of the Alfvén velocity. These waves are observed to occur in narrow regions typically of the order 1–3 km and have highly irregular waveforms [Gurnett *et al.*, 1984].

It is of interest to compare the signatures observed by the HF Doppler setup in the course of the pumping experiments on February 16 and 17, 1996, to those which were obtained during “natural” substorm events. A detailed analysis of Doppler spectrum features of diagnostic HF signals was performed by Blagoveshchenskaya *et al.* [1997] and Blagoveshchensky and Blagoveshchenskaya [1994]. It was shown that the occurrence of wave processes of different periods, associated with magnetic pulsations and internal atmospheric gravity waves, is the most typical feature of the “natural” substorm events. Sometimes, the splitting of a Doppler record into two tracks took place. Nonetheless,

the wideband spectral features and burst-like noise enhancement, closely linked to the auroral activations on February 16 and 17, 1996, have never been detected during “natural” substorm onsets.

Plate 4 presents EISCAT Tromsø UHF radar data ( $N_e$ ,  $T_e$ ,  $T_i$ , and  $V_i$ ) obtained on February 16, 1996, from 1900 to 2200 UT. In Plate 4 one can clearly see that in the first two consecutive heating cycles from 2100 to 2104 UT and 2110 to 2114 UT, an increase in the ion temperature  $T_i$  occurred in the altitude range 120–260 km was clearly observed. Recall that the HF pump wave was reflected from heights of  $\sim 100$ –110 km. It is worthwhile to consider the EISCAT UHF radar data in more detail.

Figure 10 displays the behavior of  $N_e$ ,  $T_i$ ,  $T_e$ , and  $V_i$  at an altitude of 150 km obtained on February 16, 1996, from 2030 to 2300 UT. One can see a very strong  $T_i$  increase (up to

February 16, 1996

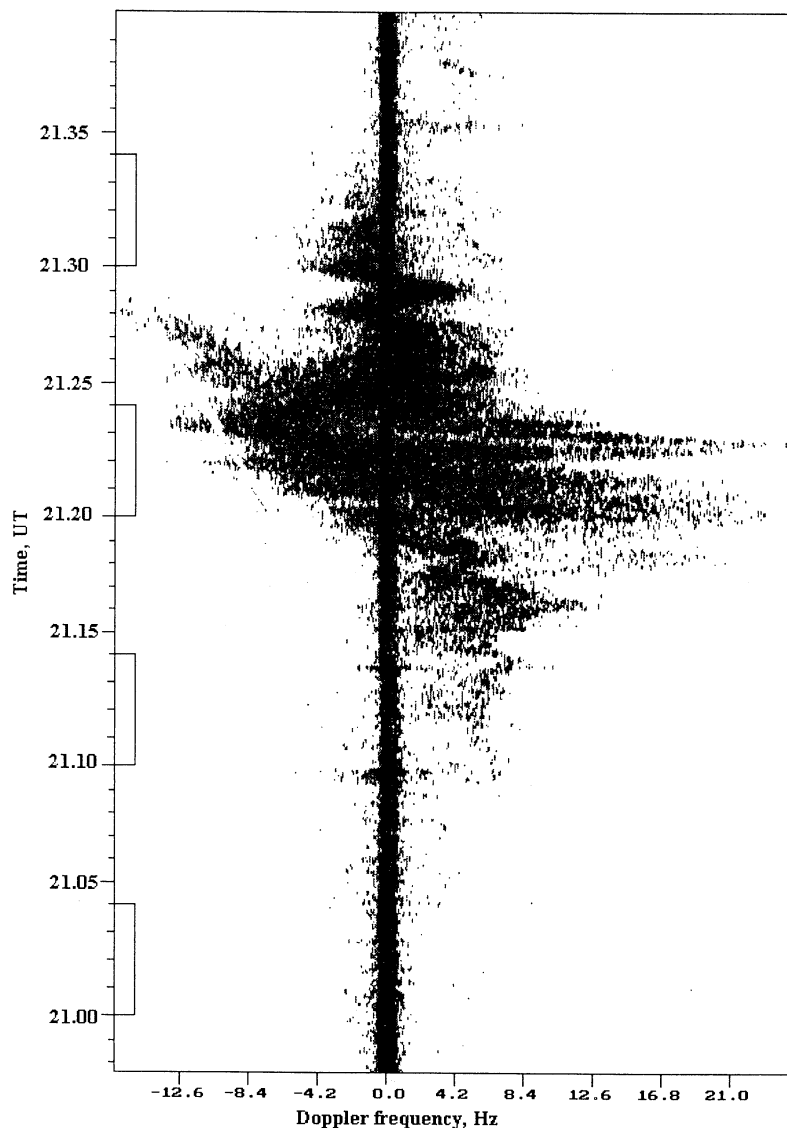


**Figure 9.** Dynamic Doppler spectra of HF diagnostic signals on the London–Tromsø–St. Petersburg path at operational frequency 9410 kHz on February 16, 1996, from 2058 to 2140 UT. The intervals when the Tromsø heater was turned on are marked on the time axis.

1800 K) closely correlated to the heater-on periods of 2100–2104 and 2110–2114 UT. Note that  $T_i$  values were  $\sim 600$  K just before the heater was turned on. Electric field data from EISCAT UHF radar tristatic measurements were also available during the experiment. An examination of the horizontal electric field measurements shows that there were drastic increases in the electric field values up to  $70 \text{ mV m}^{-1}$ , closely related to the heater-on periods at 2100–2104 UT and 2110–2114 UT.

Similar to the event of February 17, 1996, we observed in the EISCAT UHF radar data during the auroral activation onset at 2121 UT a burst-like increase of  $N_e$  at altitudes upward from 100 km. Furthermore, once started at  $\sim 2121$  UT, the process of the auroral activation development was able to maintain itself even when the heater was turned off. This can be seen from Plate 4 which exhibits an electron density

increase before 2130 UT, at which time the HF heater was turned off.

Further inspection of Figure 10 discloses that the behavior of  $T_i$ ,  $N_e$ , and  $T_e$  in later hours from 2230 UT was in much the same fashion as the changes of these parameters, which were observed from 2100 UT. A marked increase in ion temperatures  $T_i$  occurred during two consecutive heater-on periods from 2230 to 2234 UT and from 2240 to 2244 UT. Electric field measurements also showed a significant increase of up to 35 and  $60 \text{ mV m}^{-1}$  in the same pumping cycles. The electric field was directed to the south, which corresponds to a westward electrojet intensification.

The examination of the magnetic field X, Y, and Z components from the IMAGE magnetometer network (see Figure 7) showed that a new auroral activation occurred at 2240 UT exactly above Tromsø in a localized latitudinal re-

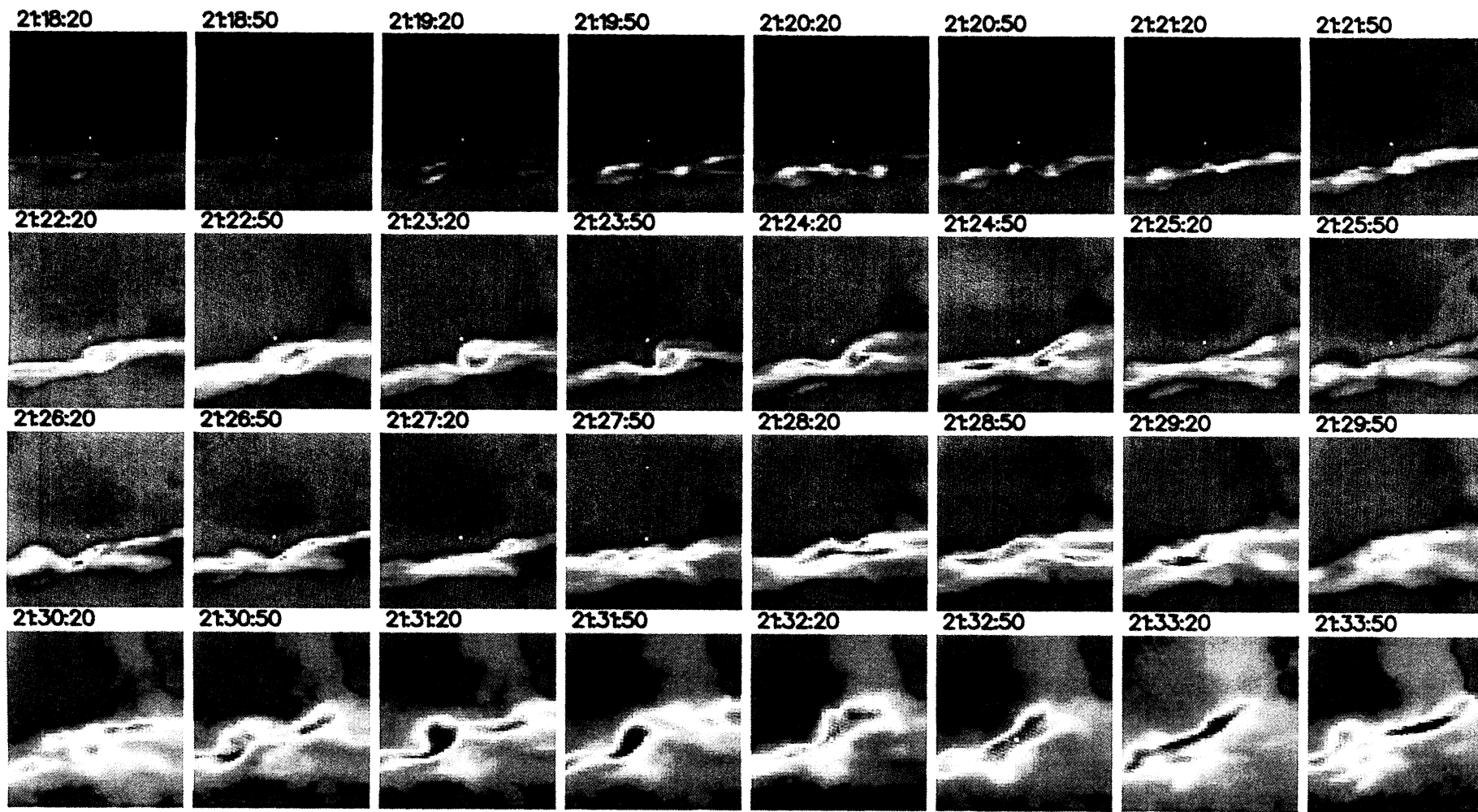


**Plate 3.** A sequence of all-sky imager plots at 557.7 nm obtained near Tromsø on February 16, 1996, from 2118:20 to 2133:50 UT. The spatial scale of each plot is the same as that in Figure 1. The plot time is 30 s. The Tromsø heater was turned on from 2120 to 2124 UT and from 2130 to 2134 UT.

# EISCAT UHF radar, Tromsø, 16 February 1996

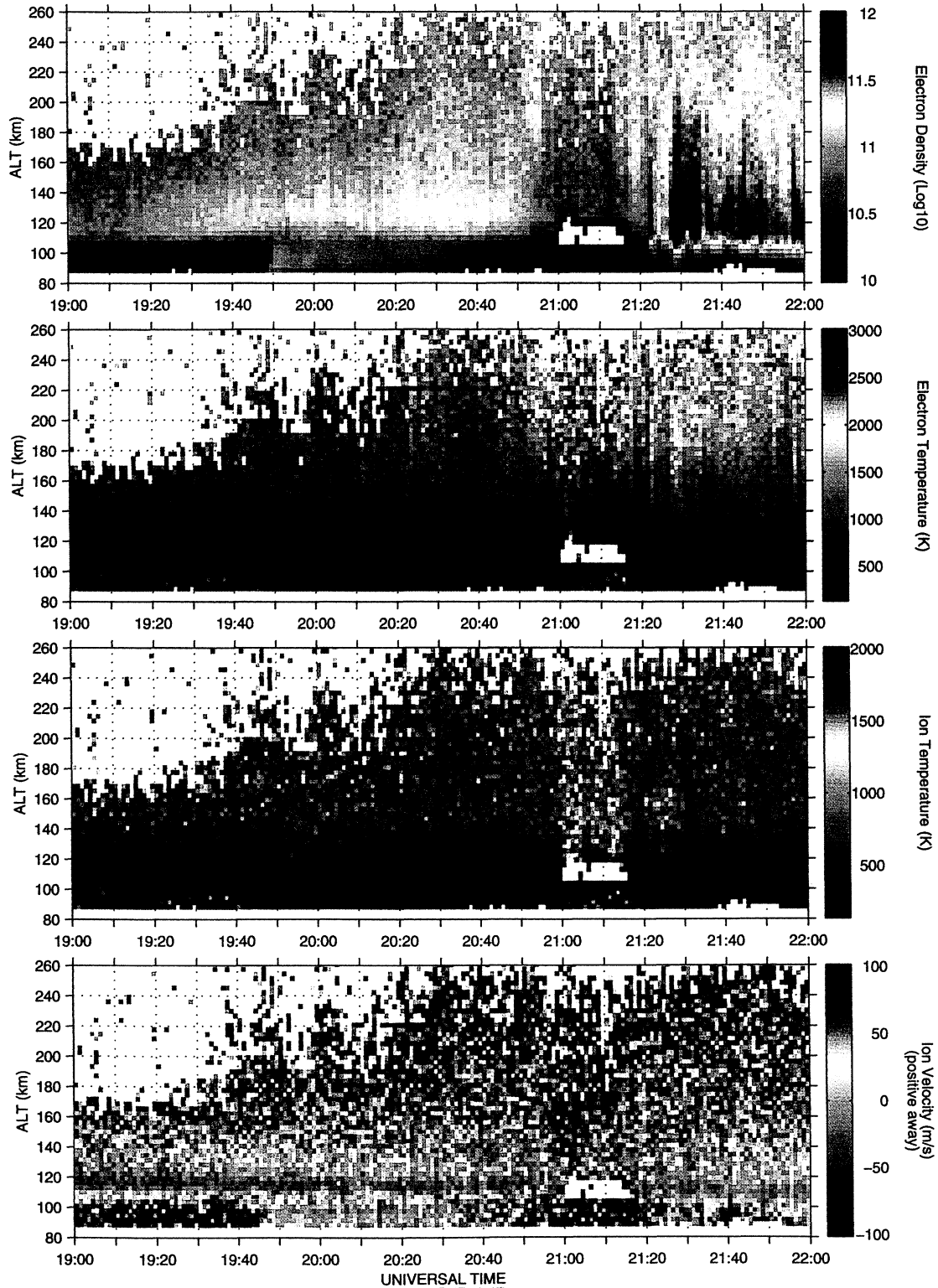


**Plate 4.** Behavior of the electron density, electron and ion temperatures, and ion velocity from Tromsø EISCAT UHF radar measurements in the field-aligned direction on February 16, 1996, from 1900 to 2200 UT obtained by the use of the high spatial resolution alternating code (AC). The interval from 2100 to 2115 UT with a “missing data layer” at ~110 km represents data which were discarded in the analysis, owing to elevated electron temperatures produced by the Farley-Buneman instability caused by large drifts (horizontal electric fields). The elevated ion temperature over the whole 120–260 km height range is evidence of such fields. All these phenomena are well recognized. The Tromsø HF heating facility was operated from 2100 to 2300 UT with a 4 min on, 6 min off pump cycle.

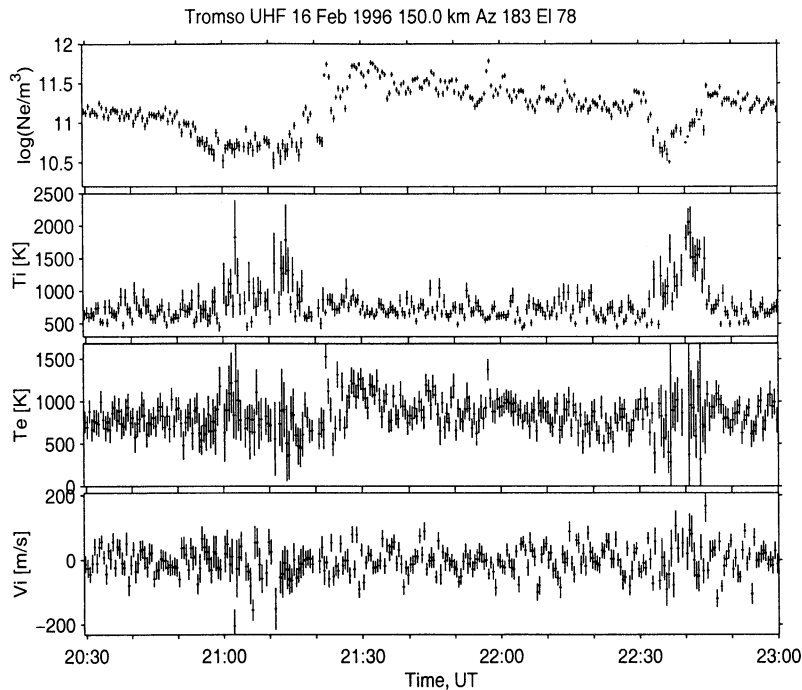


**Figure 10.** Behavior of ionospheric parameters ( $N_e$ ,  $T_i$ ,  $T_e$ , and  $V_i$ ) from Tromsø EISCAT UHF radar measurements on February 16, 1996, from 2030 to 2300 UT at the altitude of 150 km.

gion from SOR station to MAS station. This can be seen from the reversal of the  $Z$  component from positive values at SOR to negative values at MAS. Therefore, in the course of the Tromsø HF pumping experiment on February 16, 1996, two auroral activations occurred which were analogous in physical signatures and closely connected to the HF pumping of the auroral ionosphere.

From the multi-instrument experimental data on February 16, 1996, one can identify the following specific features, related to the auroral activations: (1) a modification of the auroral arc and local spiral-like formation; (2) local changes of the horizontal currents in the  $E$  region in the vicinity of Tromsø; (3) the generation of burst-like noise in the frequency range up to 35 Hz; (4) a burst-like increase in  $N_e$  at heights upward from 100 km; (5) strong increase in  $T_i$  in a wide altitude range and north-south component of electric field; (6) occurrence of two auroral activations at 2121 and 2240 UT with completely similar changes of ionospheric plasma parameters; and (7) substorm activations in the localized latitudinal region above Tromsø.

#### 4. Discussion

A bistatic HF Doppler radio scattering setup has been used in conjunction with the IMAGE magnetometer network, the DASI digital all-sky imager, the Tromsø dynasonde, the EISCAT UHF radar, and IMP 8 and IMP 9 satellites to find evidence that powerful HF radio waves can cause a modification of the ionosphere-magnetosphere coupling which can lead to a local intensification of the auroral activity. Results presented, as obtained from observations made on two consecutive nights, can be interpreted as auroral activations localized over the Tromsø HF heating facility.

In recent times, the possibility of triggering magnetospheric substorms by artificial impacts has been discussed. An artificial localization of a magnetospheric substorm by strong HF radio beams was considered by *Mogilevsky* [1999], based on measurements on board the Interball-2 (auroral probe) satellite. From a consideration of the results of active experiments, *Foster* [1998] concluded that substorm onsets may be initiated by such actions. A distinctive feature of the experiments reported here is that the HF pump waves were reflected from an auroral  $E_s$  layer. The presence of a sporadic  $E_s$  layer as well as an auroral arc in the vicinity of the Tromsø heating facility is indicative of naturally precipitating electrons with an energy of a few keV.

First of all, it should be mentioned that there are two basic possibilities to locally activate the auroral activity by an artificial ionospheric modification. The simplest one is creating such a strong perturbation that the surrounding currents exceed the threshold for an instability producing energetic electrons. It implies that the height-integrated conductivity,  $\Sigma = \alpha \int N_e(z) dz$ , be changed by a factor of 5–10 inside a region of more than 10-km dimension. This may happen during the injection of charged particle beams and plasma clouds in the ionosphere as described by *Holmgren et al.* [1980].

Another possibility, initially explored by *Zhulin et al.* [1978], is a positive feedback in the magnetosphere-ionosphere coupling during the substorm growth phase (see the different scenarios of *Kan* [1993], *Trakhtengerts and Feldstein* [1991], and *Lysak* [1991]). In this way, an artificially created conductivity perturbation in the  $E$  region grows faster than in the adjacent regions until a critical value of the field-aligned current (FAC) is reached. Note that in our Tromsø HF pumping experiments, the auroral activa-

tions were observed some 20–30 min after the start of the HF heater operation. This is a significant indication that a positive feedback mechanism in the magnetosphere-ionosphere coupling is preferred over other mechanisms to produce the local auroral activations by HF pump waves beamed into a sporadic  $E_s$  layer.

During the experiments, local changes of the ionospheric conductivities, and therefore currents in the magnetic flux tube footprinted at Tromsø, were observed. Note that the duration of the HF heater-on period was 4 min in our HF pumping experiments. In this long-period heating cycle, conductivity changes were produced owing to electron density disturbances. Their effect was much stronger than those of the short-period heating cycles [Stubbe, 1996]. Results from calculations for long-period heating cycles have shown that the conductivity perturbations in the HF pump-modified region are of the order of  $\delta\Sigma(\mathbf{r}) = 2 \text{ S}$  [Lyatsky *et al.*, 1996]. Very drastic local horizontal current changes, closely correlated with auroral activations during the heater-on periods, were seen in the behavior of the equivalent current vectors obtained from the  $X$  and  $Y$  magnetic field components obtained by the IMAGE magnetometer network (see Figures 5 and 8). It is quite possible that the region of the heater-enhanced ionospheric conductivity was polarized in the background electric field and that the polarization electric field propagated into the magnetosphere along the magnetic field lines as the field of an outgoing Alfvén wave [Lyatsky and Maltsev, 1983; Kan and Sun, 1985; Lysak, 1990; Borisov *et al.*, 1996; Kozlovsky and Lyatsky, 1997]. However, other nonlinear processes may also have contributed to the effects observed.

Another phenomenon which accompanied the auroral activations was the appearance of wideband spectral features in the Doppler radio scattering data. There are reasons to assume that these spectral features may be associated with pump-induced VLF and ELF noise. Note that these spectral features were observed when the Tromsø heating facility was operated in a 4 min on, 6 min off mode, which corresponds to frequencies which are significantly lower than that of the waves excited. Therefore the VLF and ELF noise in our experiments is not the same as the well-known effect of ELF and VLF excitation at combination frequencies [Germantsev *et al.*, 1974; Rietveld *et al.*, 1989]. The emissions observed must be of another origin. It should be pointed out that VLF and ELF noise propagating into the topside ionosphere over large distances excited by unmodulated HF pump waves were identified by Vas'kov *et al.* [1998] in satellite experiments.

It is thought that on February 17, 1996, VLF waves at the harmonics of the lower hybrid frequency were generated by the 150 MW effective radiated power (ERP) HF waves from the Tromsø heating facility. These VLF waves propagated, in the whistler mode, along the Tromsø magnetic field line into the upper ionosphere. Their interaction with natural precipitation electrons (1–10 keV) due to a cyclotron resonance led to a pump-induced precipitation of more hard electrons with energies of 10–40 keV responsible for the occurrence of an additional short-lived track on the Doppler sonogram

(see Figure 6). From the results obtained we conclude that an auroral activation exactly above Tromsø at 2033 UT was initiated by the pump-induced precipitation of the electrons.

One would expect that on February 16, 1996, Alfvén waves were excited by the powerful HF radio waves beamed into the nightside auroral  $E$  region. These Alfvén waves can be associated with the ELF noise enhancement occurring over a frequency range of up to 35 Hz (see Figure 9).

It should be noted that the amplification of the interaction between the magnetospheric convection and the ionospheric base is induced by accelerated electrons. What accelerator mechanisms can be caused by HF pumping of the base of the ionosphere at  $\sim 100 \text{ km}$ ? It is well known that the HF pump wave may excite plasma waves and turbulence in the resonant region where the ordinary mode ( $O$  mode) of the pump wave is reflected from the ionosphere and in the upper hybrid (UH) resonance region. The threshold field strength for the generation, due to ponderomotive force effects, of plasma waves by a powerful  $O$  mode radio wave is of the order  $E_{th} \approx 200 \text{ mV m}^{-1}$  [Fejer, 1979; Thidé, 1990], a value which was significantly exceeded in our experiments. As was pointed out by Fejer [1979], partial pressure effects can lower this threshold. It is known [Bernhardt *et al.*, 1988] that electrons are accelerated by the electric potential associated with plasma waves excited by HF pump waves at the plasma and upper hybrid resonance levels. HF pump-induced ohmic and anomalous heating increases the electron temperature  $T_e$  and the plasma pressure in the modified ionosphere. This leads to an electron flux transport along the magnetic field lines. HF pumping may also lead to other possible accelerator mechanisms which occur in the naturally disturbed auroral ionosphere: low-frequency plasma instabilities, kinetic Alfvén waves, and anomalous resistivity [Borovsky, 1993; Vogt and Haerendel, 1998].

Let us consider a probable chain of events during the growth phase of a substorm after a stable auroral arc has appeared and after the heater is turned on. Usually, a significant part of the upward current in the arc current system  $j_{z0}^\uparrow$  is carried by precipitating energetic electrons that ionize the ionosphere. In the positive feedback instability scenario, perturbations of the plasma density and that of the upward FAC intensity are tied as  $d(\delta N_e)/dt \simeq Q\delta j_z^\uparrow (\text{cm}^{-3} \text{ s}^{-1})$ . Here  $Q$  is the ionization function of the precipitating flux, and  $j_z^\uparrow$  is in  $\mu\text{A m}^{-2}$ .

In turn, the perturbation of  $j_z^\uparrow$  carried by an Alfvén wave, generated over a conductivity perturbation  $\delta\Sigma(\mathbf{r})$ , can be approximated as [*e.g.*, Kozlovsky and Lyatsky, 1997]

$$\delta j_z \simeq \frac{\Sigma_A}{\Sigma_p} \frac{\delta\Sigma}{\Sigma_{p0}} j_{z0}^\uparrow \simeq \beta j_{z0}^\uparrow \frac{\delta N_e}{N_e}, \quad (1)$$

where  $\Sigma_A = 1/\mu_0 V_A$  is the wave conductivity,  $\mu_0$  is the vacuum permeability,  $V_A$  is the Alfvén velocity,  $\Sigma_p$  is the height-integrated Pedersen conductivity, and  $\beta \sim 0.1$ . An initial inhomogeneity grows with a characteristic rate (instability increment) of  $\gamma \simeq Q\beta j_{z0}^\uparrow/N_e \simeq 10^{-3} \text{ s}^{-1}$  for  $Q = (3-10) \times 10^2$ ,  $N_e = 10^5 \text{ cm}^{-3}$ ,  $j_{z0}^\uparrow = 3-1$ . This implies that waves propagate toward the source of energetic particles without losses



and that their transit time is short,  $\ll \gamma^{-1}$ . Since  $\gamma^{-1}$  is small compared to the duration of the growth phase, the instability has enough time to develop. Therefore we point out that the field-aligned current-driven instability will start earlier in the region over the heater-enhanced conductivity patch in the  $E$  region of the auroral ionosphere in course of the growth phase when the FAC system is being enhanced. A positive feedback in the magnetosphere-ionosphere coupling was included so that the initial enhancement will grow until the critical FAC value is reached.

Another possible scenario is the excitation of a turbulent Alfvén boundary layer (TABL) in the ionospheric Alfvén resonator (IAR) as described by *Trakhtengerts and Feldstein* [1991]. The IAR instability increment  $\gamma$  for an arbitrary ionization value of the ionospheric  $E$  layer is expressed by [*Trakhtengerts and Feldstein*, 1991]

$$\gamma = -\frac{V_{A0}}{L} \frac{\frac{\Sigma_P}{3\Sigma_A}}{1 + \left(\frac{\Sigma_P}{3\Sigma_A}\right)^2} \left(1 - \frac{V_{th}}{V_0}\right), \quad (2)$$

where  $V_{A0}$  is the Alfvén velocity at the height of maximum plasma concentration,  $L$  is the height of the upper wall of the IAR,  $\Sigma_P$  is the height-integrated Pedersen conductivity of the ionosphere,  $\Sigma_A$  is the wave conductivity of the magnetosphere,  $V_0$  is the convection velocity, and  $V_{th}$  is the minimum threshold velocity of the convection which is necessary for an instability to develop. The main TABL parameters estimated by *Trakhtengerts and Feldstein* [1991] have the following characteristics: (1) The threshold velocity of magnetospheric convection is in the approximate range  $V_{th} \sim 100\text{--}400 \text{ m s}^{-1}$ ; (2) the basic turbulence scale length of the Alfvén waves is  $K_0 \approx 1.5 \text{ km}^{-1}$ ; and (3) the accelerated-electron energy flux density can reach  $F = 100 \text{ ergs cm}^{-2} \text{ s}^{-1}$ .

One possible IAR instability-triggering mechanism in HF pumping experiments is the change of the horizontal electric field  $E_0$  or the ratio  $\Sigma_P/3\Sigma_A$ , which determines the growth rate value (equation (2)). It has been shown that a strong local increase of  $E_0$  can occur just outside of the heater-modified ionospheric region near its nose, if the disturbed region is stretched along the background electric field  $E_0$  and the disturbance is large. In this case the amplitude of electric field  $E_m$  near the nose of the modified region can be written as [*Trakhtengerts et al.*, 2000]

$$E_m = E_0 \left(1 + \left[\frac{b}{a} + \frac{(\Sigma_{P0} + \Sigma_A) \delta \Sigma_P}{(\delta \Sigma_P)^2 + (\delta \Sigma_H)^2}\right]^{-1}\right), \quad (3)$$

where  $b$  and  $a$  are the smaller and larger half-axes of the disturbance ellipse and  $\delta \Sigma_{P,H} = \Sigma_{P,H} - \Sigma_{(P,H)0}$  are the changes of the Pedersen and Hall conductivities, respectively, due to HF pumping. It should be noted that the electric field measurements from the EISCAT UHF radar during the HF pumping experiment on February 16, 1996, clearly showed a drastic increase of the electric field closely related to the heater-on periods. Moreover, such an increase occurred in

both of the auroral activations observed during this experiment. We cannot completely exclude that electric field enhancements of this kind might be the consequence of a “natural” magnetospheric event. Nevertheless, estimates of  $E_m$  for a large heater-induced disturbance ( $\Sigma_H/\Sigma_P \approx 3$ ,  $\delta \Sigma_H/\Sigma_{H0} \approx 1$ ,  $\Sigma_A/\Sigma_{H0} \approx 0.5$ ), for  $b/a = 0.2$  give the value of the electric field amplitude of the order  $E_m \approx 3.5E_0$  [*Trakhtengerts et al.*, 2000], which is close to what we observe.

It is believed that Alfvén wave generation and electric field enhancement during HF pump experiments provide a possibility for an instability excitation in the IAR, bounded from below by the pump-modified ionospheric  $E$  region and from above by the region of sharp increase of Alfvén velocities at heights up to one Earth radius. The TABL consists of small-scale Alfvén vortices ( $l \approx 1\text{--}3 \text{ km}$ ) trapped inside IARs. The accumulation of energy in the magnetospheric tail is accompanied by an increase in the laminar magnetospheric convection, which, under specific geophysical conditions, can turn into a turbulent state. This mechanism would come into play through the local “switch-on” of the TABL in the selected magnetic flux tube footprinted at Tromsø, due to the dependence of the TABL excitation conditions on the ionospheric  $E$  layer.

The local “switch-on” of the turbulent boundary layer may promote the formation of a local magnetospheric current system. This would consist of two field-aligned sheet currents on the northward and southward sides of the heater-modified auroral  $E$  region closed via Pedersen currents in the ionosphere. The configuration of this current system is similar to the second configuration (Type II) of *Boström’s* [1964] model with driving forces inside this system. In addition, it drives a Hall current. The formation of a local magnetospheric current system is confirmed by the behavior and features of the auroral arc near Tromsø. From optical data obtained during heater-on periods, the appearance of the local spiral-like or bulge structures in the auroral arcs, typical for the region of the field-aligned currents, can be clearly identified in the vicinity of Tromsø (Figures 2 and 7).

## 5. Summary

Experimental results from multi-instrument observations during Tromsø HF pumping experiments in the nightside auroral  $E$  region indicate that the localization and timing of the auroral activations were related to the injection of powerful HF radio waves transmitted from the Tromsø heating facility. The modification of the ionosphere-magnetosphere coupling leading to the local intensification of the auroral activity may be attributed to the following facts:

1. The transmitted  $O$  mode “heater” waves reflected from the auroral  $E$  region give rise to an increase of the ionospheric conductivity in the HF pump-modified  $E$  region. The field-aligned current-driven instability will start earlier in the region over the heater-enhanced conductivity patch during the growth phase of the auroral substorm when the FAC system is being enhanced. A positive feedback in the magnetosphere-ionosphere coupling was included in order

for the initial enhancement to grow further on until the critical value of the FAC was reached.

2. Excitation of a turbulent Alfvén boundary layer (TABL) can take place under specific geophysical conditions. The TABL consists of small-scale ( $l \approx 1\text{--}3$  km) Alfvén vortices trapped inside an ionospheric Alfvén resonator which is bounded from the bottom by the HF pump-modified  $E$  region and from the top by the region of sharp increase in the Alfvén velocity at altitudes up to one Earth radius. The local “switch-on” of the TABL in the selected magnetic tube can turn the laminar magnetospheric convection into a turbulent state.

3. The local “switch-on” of the TABL may promote the formation of a local magnetospheric current system. It consists of two field-aligned sheet currents on the northward and southward sides of the heater-modified auroral  $E$  region, closed via Pedersen currents in the ionosphere.

4. The triggering of local auroral activations by HF pump waves requires specific geophysical conditions, namely, the presence of the accumulation of energy in the magnetospheric tail. The accumulation of energy is accompanied by an increase of the laminar convection, which manifests itself in the growth of the electric field, formation of the auroral electrojet, etc. In this manner the energy source for the auroral activations remains the interaction between the solar wind and the magnetosphere.

We conclude that the experimental results presented here prove the active role of the ionosphere in a substorm process and provide intriguing evidence that the injection of a powerful HF radio beam into an auroral sporadic  $E$  layer may cause the triggering of local auroral activations. Therefore further experiments of the same controlled repeatable character are called for.

**Acknowledgments.** We would like to thank the Director and Staff of the EISCAT Scientific Association for providing the radar data. EISCAT is an International Association supported by Finland (SA), France (CNRS), the Federal Republic of Germany (MPG), Japan (NIPR), Norway (NFR), Sweden (NFR), and the United Kingdom (PPARC). The work of the first three Russian authors (N. B., V. K., and T. B.) was supported by grants from the Swedish Institute (SI) within the Visby Programme and from the Royal Swedish Academy of Sciences (KVA). They are also grateful to the Russian Foundation of Fundamental Research, grants 97-05-65443 and 00-05-64819. The Swedish author gratefully acknowledges financial support from the Swedish Natural Sciences Research Council (NFR). The first two authors (N.B. and V.K.) and the sixth author (M.R.) were partly supported by NATO linkage grant CLG 975069. The IMAGE magnetometer data used in this paper were collected as a German-Finnish-Norwegian-Polish-Russian-Swedish project conducted by the Finnish Meteorological Institute. The first three Russian authors wish to thank the Swedish Institute of Space Physics (Uppsala Division) for the assistance and hospitality they enjoyed during their visit there. The authors thank Rolf Boström, Thomas Leyser, Tobia Carozzi, Kristof Stasiewicz, and Victor Trakhtengerts for useful discussions and helpful comments.

Michel Blanc thanks Dennis Papadopoulos and another referee for their assistance in evaluating this paper.

## References

- Akasofu, S.-I., The development of the auroral substorm, *Planet. Space Sci.*, **12**, 273–282, 1964.
- Bernhardt, P. A., L. M. Duncan, and C. A. Tepley, Artificial airglow excited by high-power radio waves, *Science*, **242**, 1022–1027, 1988.
- Blagoveshchensky, D. V., and N. F. Blagoveshchenskaya, Wave disturbances in high latitudinal ionosphere during substorm (in Russian), *Geomagn. Aeron.*, **34**, 87–96, 1994.
- Blagoveshchenskaya, N. F., V. J. Vovk, V. A. Kornienko, and I. V. Moskvina, Wave processes in high latitudinal ionosphere observed from radiophysical measurements (in Russian), *Geomagn. Aeron.*, **37**, 70–78, 1997.
- Blagoveshchenskaya, N. F., V. A. Kornienko, A. V. Petlenko, A. Brekke, and M. T. Rietveld, Geophysical phenomena during an ionospheric modification experiment at Tromsø, *Ann. Geophys.*, **16**, 1212–1225, 1998.
- Blagoveshchenskaya, N. F., V. A. Kornienko, A. Brekke, M. T. Rietveld, M. J. Kosch, T. D. Borisova, and M. V. Krylov, Phenomena observed by HF long-distance tools in the HF modified auroral ionosphere during magnetospheric substorm, *Radio Sci.*, **34**, 715–724, 1999.
- Borisov, N., A. Gurevich, K. Papadopoulos, and C. L. Chang, Controlled generation of coherent low frequency ULF/ELF/VLF, *Radio Sci.*, **31**, 859–867, 1996.
- Borovsky, J. E., Auroral arc thicknesses as predicted by various theories, *J. Geophys. Res.*, **98**, 6101–6111, 1993.
- Bösinger, T., K. Kaila, R. Rasinkangas, P. Pollari, J. Kangas, V. Trakhtengerts, and A. Demekhov, An EISCAT study of a pulsating auroral arc: Simultaneous ionospheric electron density, auroral luminosity and magnetic field pulsations, *J. Atmos. Terr. Phys.*, **58**, 23–35, 1996.
- Boström, R., A model of the auroral electrojets, *J. Geophys. Res.*, **69**, 4983–4999, 1964.
- Djuth, F. T., et al., Observations of  $E$  region irregularities generated at auroral latitudes by a high power radio wave, *J. Geophys. Res.*, **90**, 12,293–12,306, 1985.
- Fejer, J. A., Ionospheric modification and parametric instabilities, *Rev. Geophys.*, **17**, 135–153, 1979.
- Foster, J. C., Substorm onset associated with active experiments, paper presented at *International conference on Substorms-4*, Solar-Terrestrial Environment Laboratory (STEL), Lake Hamana, Japan, 1998.
- Getmantsev, G. G., N. A. Zujkov, D. S. Kotik, L. P. Mironenko, N. A. Mityakov, and V. O. Rapoport, Combination frequencies in the interaction between high-power short-wave radiation and ionospheric plasma, *JETP Lett.*, **20**, 101–102, 1974.
- Gurnett, D. A., R. L. Huff, J. D. Menietti, J. L. Burch, and J. D. Winningham, Correlated low-frequency electric and magnetic noise along the auroral field lines, *J. Geophys. Res.*, **89**, 8971–8985, 1984.
- Haerendel, G., Field-aligned currents in the Earth’s magnetosphere, in *Physics of Magnetic Flux Ropes*, *Geophys. Monogr. Ser.*, vol. 58, pp. 539–553, AGU, Washington, DC, 1990.
- Henderson, M. G., G. D. Reeves, R. D. Belian, and J. S. Murphree, Observations of magnetospheric substorms occurring with no apparent solar wind/IMF trigger, *J. Geophys. Res.*, **101**, 10,773–10,791, 1996.
- Holmgren, G., R. Boström, M. C. Kelley, P. M. Kintner, R. Lundin, U. V. Fahlson, E. A. Bering, and W. R. Sheldon, Trigger: An active release experiment that stimulated auroral particle precipitation and wave emissions, *J. Geophys. Res.*, **85**, 5043–5053, 1980.
- Kamide, Y., and W. Baumjohann, *Magnetosphere-Ionosphere Coupling*, Springer-Verlag, New York, 1993.
- Kan, J., On the cause of substorm expansion onset and the processes driving the substorm expansion phase, *J. Atmos. Terr. Phys.*, **55**, 979–983, 1993.
- Kan, J. R., and W. Sun, Simulation of the westward traveling surge and Pi2 pulsation during substorms, *J. Geophys. Res.*, **90**, 10,911–10,922, 1985.
- Kosch, M. J., T. Hagfors, and E. Nielsen, A new digital all-sky imager experiment for optical auroral studies in conjunction with

- Scandinavian twin auroral radar experiment, *Rev. Sci. Instrum.*, **69**, 578–584, 1998.
- Kozlovsky, A. E., and W. B. Lyatsky, Alfvén wave generation by disturbance of ionospheric conductivity in the field-aligned current region, *J. Geophys. Res.*, **102**, 17,297–17,303, 1997.
- LaBelle, J., M. L. Trimpi, R. Brittain, and A. T. Weatherwax, Fine structure of auroral roar emissions, *J. Geophys. Res.*, **100**, 21,953–21,959, 1995.
- Leyser, T. B., B. Thidé, M. Waldenvik, E. Veszelei, V. L. Frolov, S. M. Grach, and G. P. Komrakov, Downshifted maximum features in stimulated electromagnetic emission, *J. Geophys. Res.*, **99**, 19,555–19,568, 1994.
- Lühr, H., A. Aylward, S. C. Buchert, A. Pajunpää, T. Holmboe, and S. M. Zalewski, Westward moving dynamic substorm features observed with the image magnetometer network and other ground-based instruments, *Ann. Geophys.*, **16**, 425–440, 1998.
- Lui, A. T., and J. S. Murphree, A substorm model with onset location tied to an auroral arc, *Geophys. Res. Lett.*, **25**, 1269–1272, 1998.
- Lundborg, B., and B. Thidé, Standing wave pattern of HF radio waves in the ionospheric reflection region, 2, Applications, *Radio Sci.*, **21**, 486–500, 1986.
- Lyatsky, W. B., and Y. P. Maltsev, *The Magnetosphere-Ionosphere Interaction*, Nauka, Moscow, 1983.
- Lyatsky, W. B., E. G. Belova, and A. B. Pashin, Artificial magnetic pulsation generation by powerful ground-based transmitter, *J. Atmos. Terr. Phys.*, **58**, 407–417, 1996.
- Lysak, R. L., Electrodynamic coupling of the magnetosphere and ionosphere, *Space Sci. Rev.*, **52**, 33–87, 1990.
- Lysak, R. L., Feedback instability of the ionospheric resonant cavity, *J. Geophys. Res.*, **96**, 1553–1568, 1991.
- Lysak, R. L., and Y. Song, Dynamics of auroral arc formation during substorms, paper presented at *International conference on Substorms-4*, Solar-Terrestrial Environment Laboratory (STEL), Lake Hamana, Japan, 1998.
- McPherron, R. L., C. T. Russell, and M. P. Aubry, Satellite studies of magnetospheric substorms on August 15, 1968, 9, Phenomenological model for substorms, *J. Geophys. Res.*, **78**, 3131–3149, 1973.
- Mogilevsky, M., Artificial localization of magnetospheric substorms by a HF heating facility, paper presented at *International Conference Dynamics of the Magnetosphere and its Coupling to the Ionosphere on Multiple Scales From INTERBALL, ISTP Satellites and Ground-Based Observations*, Space Research Institute (IKI) of the Russian Academy of Sciences, Zvenigorod, Russia, 1999.
- Nagatsuma, T., H. Fucunishi, H. Hayakawa, T. Mucai, and A. Matsuo, Field-aligned currents associated with Alfvén waves in the poleward boundary region of the nightside auroral oval, *J. Geophys. Res.*, **101**, 21,715–21,729, 1996.
- Noble, S. T., et al., Multiple frequency radar observations of high-latitude E region irregularities in the HF modified ionosphere, *J. Geophys. Res.*, **92**, 13,613–13,627, 1987.
- Rietveld, M., P. Stubbe, and H. Kopka, On the frequency dependence of ELF/VLF waves produced by modulated ionospheric heating, *Radio Sci.*, **24**, 270–278, 1989.
- Rietveld, M., H. Kohl, H. Kopka, and P. Stubbe, Introduction to ionospheric heating at Tromsø, 1, Experimental overview, *J. Atmos. Terr. Phys.*, **55**, 577–599, 1993.
- Rishbeth, H., and T. van Eyken, EISCAT: Early history and the first ten years of operation, *J. Atmos. Terr. Phys.*, **55**, 525–542, 1993.
- Rostoker, G., The evolving concept of a magnetospheric substorm, *J. Atmos. Terr. Phys.*, **61**, 85–100, 1999.
- Rostoker, G., S.-I. Akasofu, W. Baumjohann, Y. Kamide, and R. L. McPherron, The roles of direct input of energy from the solar wind and unloading of stored magnetotail energy in driving magnetospheric substorms, *Space Sci. Rev.*, **46**, 93–111, 1987.
- Samson, J. C., L. L. Cogger, and Q. Pao, Observations of field line resonances, auroral arcs, and auroral vortex structures, *J. Geophys. Res.*, **101**, 17,373–17,383, 1996.
- Stasiewicz, K., et al., Small scale Alfvénic structure in the aurora, *Space Sci. Rev.*, **92**, 423–533, 2000.
- Stubbe, P., Review of ionospheric modification experiments in Tromsø, *J. Atmos. Terr. Phys.*, **58**, 349–368, 1996.
- Stubbe, P., H. K. B. Thidé, and H. Derblom, Stimulated electromagnetic emission: A new technique to study the parametric decay instability in the ionosphere, *J. Geophys. Res.*, **89**, 7523–7536, 1984.
- Thidé, B., Stimulated scattering of large amplitude waves in the ionosphere: Experimental results, *Phys. Scr.*, **T30**, 170–180, 1990.
- Thidé, B., H. Kopka, and P. Stubbe, Observations of stimulated scattering of a strong high-frequency radio wave in the ionosphere, *Phys. Rev. Lett.*, **49**, 1561–1563, 1982.
- Thidé, B., H. Derblom, Å. Hedberg, H. Kopka, and P. Stubbe, Observations of stimulated electromagnetic emissions in ionospheric heating experiments, *Radio Sci.*, **18**, 851–859, 1983.
- Thidé, B., Å. Hedberg, J. A. Fejer, and M. P. Sulzer, First observations of stimulated electromagnetic emission at Arecibo, *Geophys. Res. Lett.*, **16**, 369–372, 1989.
- Trakhtengerts, V. Y., and A. Y. Feldstein, Turbulent Alfvén boundary layer in the polar ionosphere, 1, Excitation conditions and energetics, *J. Geophys. Res.*, **96**, 19,363–19,372, 1991.
- Trakhtengerts, V. Y., P. P. Belyaev, S. V. Polyakov, A. G. Demekhov, and T. Bösinger, Excitation of Alfvén waves and vortices in the ionospheric Alfvén resonator by modulated powerful radiowaves, *J. Atmos. Terr. Phys.*, **62**, 267–276, 2000.
- Trefall, H., et al., Morphology and fine time structure of an early-morning electron precipitation event, *J. Atmos. Terr. Phys.*, **37**, 83–105, 1975.
- Vas'kov, V. V., N. I. Bud'ko, A. V. Kapustina, N. A. Ryabova, G. L. Gdalevich, G. P. Komrakov, and A. N. Maresov, Detection on the Intercosmos-24 satellite of VLF and ELF waves stimulated in the topside ionosphere by the heating facility 'Sura', *J. Atmos. Terr. Phys.*, **60**, 1261–1274, 1998.
- Vogt, J., and G. Haerendel, Reflection and transmission of Alfvén waves at the auroral acceleration region, *Geophys. Res. Lett.*, **25**, 277–280, 1998.
- Weatherwax, A. T., J. LaBelle, M. L. Trimpi, and R. A. Treumann, Statistical and case studies of radio emissions observed near  $2f_{ce}$  and  $3f_{ce}$  in the auroral zone, *J. Geophys. Res.*, **100**, 7745–7757, 1995.
- Zhulin, I. A., V. M. Mishin, E. Mishin, and V. M. Chmyrev, Possibility of artificial localization of a magnetospheric substorm, *Geomagn. Aeron., Engl. Transl.*, **18**, 377–378, 1978.

N. F. Blagoveshchenskaya, T. D. Borisova, V. A. Kornienko, R. Y. Luk'yanova, and O. A. Troshichev, Arctic and Antarctic Research Institute, 38 Bering Street, St. Petersburg 199 397, Russia. (natally@aari.nw.ru, vikkorn@aari.nw.ru, olegtro@aari.nw.ru)

M. J. Kosch and M. T. Rietveld, Max-Planck-Institut für Aeronomie, Max-Planck-Str. 2, D-37191 Katlenburg-Lindau, Germany. (kosch@linmpi.mpg.de, rietveld@linmpi.mpg.de)

E. V. Mishin, MIT Haystack Observatory, Westford, MA 01886. (evm@haystack.mit.edu)

B. Thidé, Swedish Institute of Space Physics, Uppsala Division, Box 537, SE-751 21 Uppsala, Sweden. (bt@irfu.se)

(Received July 5, 1999; revised December 6, 2000; accepted December 13, 2000.)